2016 IEEE 55th Conference on Decision and Control (CDC)
ARIA Resort & Casino
December 12-14, 2016, Las Vegas, USA

Singularly perturbed phase response curves for relaxation oscillators

Pierre Sacré and Alessio Franci

Abstract— **We exploit a novel geometric method to construct the global isochrones of relaxation oscillators and the associated phase response curve. This method complements the classical infinitesimal (local) phase response curve approach by constructively predicting the finite phase response curve near the singular limit of infinite timescale separations between the oscillator variables. We illustrate the power of our construction on the FitzHugh-Nagumo model of neuronal spike generation. Because of its global and constructive nature, not requiring extensive numerical simulations, the proposed approach is particularly suited to control design applications.**

I. Introduction

The phase response curve (PRC) characterizes the input–output behavior of oscillatory systems [1], [2]. It has wide applications ranging from oscillator control [3], [4] to the analysis of oscillator network synchronization [5], [6]. Systematic and analytic prediction of an oscillator phase response curve is a hard task in general and it can be accomplished only in very specific cases. This usually leads to intense case-specific numerical investigations, which might weaken the relevance of phase response curve approach in control design.

The classical approach relies on numerically computing the infinitesimal, that is, linearized, phase response curve and then use convolution to compute the phase response curve for generic inputs [7]. Whereas this linearized approach provides accurate predictions when the oscillatory behavior is quasi-harmonic or when inputs are weak, its predictive power breaks down when the oscillatory behavior becomes highly nonlinear due to timescale separation between the oscillator variables, corresponding to the relaxation oscillation limit [8].

To overcome these limitations, we use a fully nonlinear approach to study geometrically the global structure of relaxation oscillator isochrones. Our main analysis tool is geometric singular perturbation theory [9], [10]. Based on this analysis we derived semi-analytic formulas to predict the finite phase response curve to arbitrary inputs in the highly nonlinear relaxation regime. As opposed to the infinitesimal phase response curve approach, our method ensures that the error between the real and the predicted phase response curve goes to zero as the time-scale separation increases, independently of the input size, and its constructive nature makes it particularly useful in control design applications.

Although we do not provide rigorous proofs, the method is thoroughly illustrated by constructing the singular phase response curve of a generic relaxation oscillator to impulses and square pulses of finite duration. (Rigorous proofs will be developed in future works). This methodology was firstly presented in the first author Ph.D. dissertation [11] and was subsequently adapted in [12] to study the phase response curve of a specific class of hybrid reset oscillators. These results are a first step toward a geometric theory for finite phase response curves of singularly perturbed oscillators, including three-timescale bursters [13].

This work was supported by a Fulbright Belgium research scholarship awarded to P. S. and by a DGAPA-UNAM PAPIIT grant IA105816 awarded to A. F. This paper presents research results of the Belgian Network DYSCO (Dynamical Systems, Control, and Optimization), funded by the Interuniversity Attraction Poles Programme, initiated by the Belgian State, Science Policy Office. The scientific responsibility rests with its authors.

P. Sacré is with the Department of Biomedical Engineering, The Johns Hopkins University, Baltimore, MD 21218 (p.sacre@jhu.edu).

A. Franci is with the Department of Mathematics, National Autonomous University of Mexico (UNAM), 04510, Coyoacán, Ciudad de México, México (afranci@ciencias.unam.mx).

II. Relaxation oscillators and their geometry

We consider a two-dimensional fast-slow dynamical system of the form

$$\dot{x} = \quad f(x) - z + u, \tag{1a}$$
$$\dot{z} = \epsilon\, g(x, z), \tag{1b}$$

where $\dot{}$ denotes differentiation with respect to the time t, $(x, z) \in \mathbb{R}^2$, $u \in \mathbb{R}$, and $0 < \epsilon \ll 1$. The solution at time t to the initial value problem (1) from the initial condition $(x_0, z_0) \in \mathbb{R}^2$ at time 0 is denoted by $\phi^\epsilon_{\mathrm{f}}(t, (x_0, z_0), u(\cdot))$, with $\phi^\epsilon_{\mathrm{f}}(0, (x_0, z_0), u(\cdot)) = (x_0, z_0)$. In the slow time scale $\tau := \epsilon\, t$, dynamics (1) become

$$\epsilon\, x' = f(x) - z + u, \tag{2a}$$
$$z' = g(x, z), \tag{2b}$$

where $'$ denotes differentiation with respect to the slow time τ. For $\epsilon \neq 0$, (1) and (2) are equivalent. We call (1) the fast dynamics and (2) the slow dynamics. In the singular limit $\epsilon \to 0$, we obtain from (1) and (2) the *layer* dynamics

$$\dot{x} = f(x) - z + u, \tag{3a}$$
$$\dot{z} = 0, \tag{3b}$$

describing the fast evolution far from the critical manifold $\mathcal{S}^0 := \big\{(x, z) \in \mathbb{R}^2 : f(x) - z + u = 0\big\}$, and the *reduced* dynamics

$$0 = f(x) - z + u, \tag{4a}$$
$$z' = g(x, z), \tag{4b}$$

describing the slow evolution along $\mathcal{S}^0$.

Under some mild technical assumptions [10, Theorem 2.1], in particular that the critical manifold $\mathcal{S}^0$ is S-shaped, the zero-input system (1) has a unique periodic orbit γ^ϵ sliding along the stable branches of $\mathcal{S}^0$ and shadowing the singular periodic orbit γ^0 illustrated in Figure 1. The singular periodic

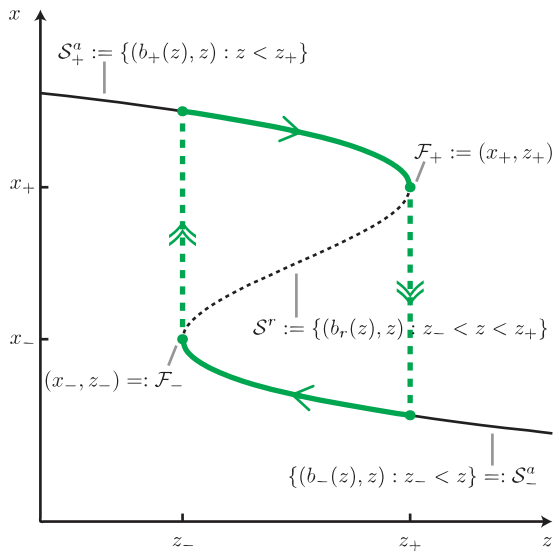

Fig. 1. Geometry of relaxation oscillators. The critical manifold $\mathcal{S}^0$ is a S-shaped curve. Under some technical assumptions [10], the system (1) in the singular limit ($\epsilon \to 0$) admits a singular periodic orbit γ^0 defined as the union of two pieces of the critical manifold associated with a slow evolution (green solid arrows) and two critical fibers associated with jumps (green dashed arrows).

orbit γ^0 is defined as the union of two pieces of the critical manifold associated with a slow evolution and two critical fibers associated with jumps. Many notations used in this paper about the geometry of relaxation oscillators are defined in Figure 1.

Remark 1: In the slow time scale, the singularly perturbed period $T^\epsilon_{\rm s}$ converges towards the singular period $T^0_{\rm s}$, which is equal to the finite time required to slide along both portions of the critical manifold (jumps are instantaneous), that is, $\lim_{\epsilon\to 0} T^\epsilon_{\rm s} =: T^0_{\rm s}$. In the fast time scale, the singularly perturbed period $T^\epsilon_{\rm f}$ blows up to infinity, that is, $\lim_{\epsilon\to 0} T^\epsilon_{\rm f} =: T^0_{\rm f}$, with $\lim_{\epsilon\to 0} T^\epsilon_{\rm f} = \lim_{\epsilon\to 0} T^\epsilon_{\rm s}/\epsilon = +\infty$. The corresponding angular frequencies are denoted $\omega^\epsilon_{\rm f} = 2\pi/T^\epsilon_{\rm f}$ and $\omega^\epsilon_{\rm s} = 2\pi/T^\epsilon_{\rm s}$.

III. Phase map and phase response curves

In this section, we introduce the concepts of phase map and phase response curves following the terminology of [1] and [2]. The interested reader is referred to [7] for details.

A. Phase map and isochrons

Because of the periodic nature of its steady-state behavior, it is appealing to study the oscillator dynamics on the unit circle $\mathbb{S}^1$. The key ingredients of this phase reduction are the concepts of phase map and isochrons.

The (asymptotic) *phase map* $\Theta^\epsilon : \mathcal{B}(\gamma^\epsilon) \subseteq \mathbb{R}^2 \to \mathbb{S}^1$ is a mapping that associates to every point in the basin of attraction $\mathcal{B}(\gamma^\epsilon)$ a phase on the unit circle $\mathbb{S}^1$. It is defined in such a way that the phase variable $\theta(t) := \Theta^\epsilon(\phi^\epsilon_{\rm f}(t, (x_0, z_0), u(\cdot)))$, that is, the image of the flow through the phase map, linearly increases with time in the case of zero inputs, $u(\cdot) \equiv 0$.

The *isochron* $\mathcal{I}^\epsilon(\theta)$ is the set of all points in $\mathcal{B}(\gamma^\epsilon)$ that are mapped to the same phase θ by the phase map $\Theta^\epsilon(\cdot)$, that is, isochrones are level sets of the phase map. Points on the same isochron asymptotically converge to the same trajectory on the periodic orbit.

B. Phase response curves

An input $u(\cdot)$ is *phase-resetting* if the solution of (1) forced by $u(\cdot)$ asymptotically converges to the periodic orbit.

The *(finite) phase response curve* $Q^\epsilon(\theta; u(\cdot)) : \mathbb{S}^1 \to [-\pi, \pi)$ associates to each phase the asymptotic phase shift of system (1) in response to a phase-resetting input $u(\cdot)$.

The *infinitesimal phase response curve* $q^\epsilon(\theta) : \mathbb{S}^1 \to \mathbb{R}$ is the relative asymptotic phase shift of system (1) in response to an infinitesimal phase-resetting impulse (Dirac δ function), that is, $q^\epsilon(\theta) := \lim_{\alpha\to 0} Q^\epsilon(\theta; \alpha\,\delta(\cdot))/\alpha$.

IV. Limitation of the infinitesimal approximation for finite phase response curves

We now briefly recall the limitation of the *infinitesimal* (local) approximation for *finite* (global) phase response curves of relaxation oscillators.

In the classical approach [1], [2], [14], the (finite) phase response curve is approximated by the "convolution" between the infinitesimal phase response curve and the input

$$Q^\epsilon(\theta; u(\cdot)) = \underbrace{\int_0^{+\infty} q^\epsilon(\omega\, s + \theta)\, u(s)\, ds}_{:= Q^\epsilon_{\rm inf}(\theta; u(\cdot))} + \mathcal{O}(\|u(\cdot)\|^2)$$

(see [7] for details about the derivation of this expression).

Because of its local/linearized nature, this approximation is only valid for inputs that are much smaller than the singular perturbation parameter, that is, $0 < \|u(\cdot)\| \ll \epsilon \ll 1$ (see [8] for details). In other words, the domain of validity of this approximation vanishes in the singular limit ($\epsilon \to 0$).

Intuitively, this limitation comes from the fact that, the singular trajectory forced by the input $u(\cdot)$ might jump instantaneously from one branch of the critical manifold to the other. This behavior involves a global phenomenon that cannot be captured by a local approximation.

V. Singularly perturbed phase response curve

The main idea of our approach is to take advantage of time-scale separation to construct the *finite* phase response curve in the singular limit. For a sufficiently small singular parameter $0 < \epsilon \ll 1$, the *singularly perturbed* finite phase response curve $Q^\epsilon(\theta; u(\cdot))$ can naturally be approximated by a *singular* finite phase response curve $Q^0(\theta; u(\cdot))$, that is,

$$Q^\epsilon(\theta; u(\cdot)) = Q^0(\theta; u(\cdot)) + \mathcal{O}\left(\epsilon^\beta\right),$$

for any phase-resetting input $u(\cdot)$ and with $0 < \beta \leq 1$. The singular phase response curve $Q^0(\theta; u(\cdot))$ is to the singularly perturbed phase response curve $Q^\epsilon(\theta; u(\cdot))$ what the singular periodic orbit in Figure 1 is to the relaxation oscillator limit cycle. In both cases, geometric singular perturbation arguments let $\beta \sim 2/3$ [10]. A rigorous proof of this claim is out of the scope of this paper and will be developed in future works. To fix the ideas, the resulting trade-off between the infinitesimal approximation and the singular approximation as

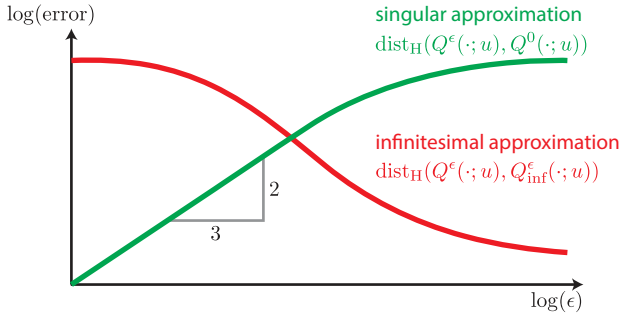

Fig. 2. Qualitative trade-off between the infinitesimal approximation and the singular approximation as a function of the time-scale separation ϵ. Errors between the actual phase response curve and its approximations are measured using the Hausdorff distance $\mathrm{dist}_{\mathrm{H}}(\cdot,\cdot)$.

a function of the time-scale separation ϵ is sketched qualitatively in Figure 2.

The remainder of the section is devoted to geometrically construct the singular phase response curve for a relaxation oscillator in the two important cases in which the input is given by *(i)* impulses, that is, $u(t) = \alpha\,\delta(t)$, and *(ii)* square pulses of finite duration, that is, $u(t) = \bar{u}\,[1_+(t) - 1_+(t-\Delta)]$.

A. Singular phase map and isochrons

A first step towards the prediction of singular (finite) phase response curves is the geometric construction of the phase map and isochrons for the system (1) in the singular limit. The construction (sketched in Figure 3) relies on the fast-slow limiting dynamics (3)–(4), in full analogy with geometric singular perturbations methods.

The singular phase map is the phase map of the singular periodic orbit. Since the singular periodic orbit γ^0 is a one-dimensional piece-wise smooth curve in $\mathbb{R}^2$, it is naturally parameterized in terms of a single scalar phase on the unit circle $\mathbb{S}^1$. As in the nonsingular case, the singular phase map is chosen such that the phase variable linearly increases with time.

We choose to associate the zero-phase reference position on the singular periodic orbit with the lower fold (x_-, z_-), that is $\Theta^0(x_-, z_-) =: \theta_- = 0$. As jumps are instantaneous in the singular limit, all points of the (weakly) unstable critical fiber joining (x_-, z_-) to $(b_+(z_-), z_-)$ are also associated with a phase equal to zero.

For points on the singular limit cycle, the phase θ associated with a point (x, z) is the normalized fraction of (slow) time $\omega_{\mathrm{s}}^0\,\Delta\tau$ needed to reach this point along the reduced dynamics (4) flow from the reference initial condition. For a point (x_1, z_1) on the upper branch, the phase will be given by

$$\Theta^0(x_1, z_1) := \omega_{\mathrm{s}}^0\,\Delta\tau_1.$$

For a point (x_2, z_2) on the lower branch, the phase will be given by

$$\Theta^0(x_2, z_2) := \omega_{\mathrm{s}}^0\,\Delta\tau_+ + \omega_{\mathrm{s}}^0\,\Delta\tau_2\,,$$

where the first term corresponds to the flowing time on the upper branch (up to the upper fold) and the second term

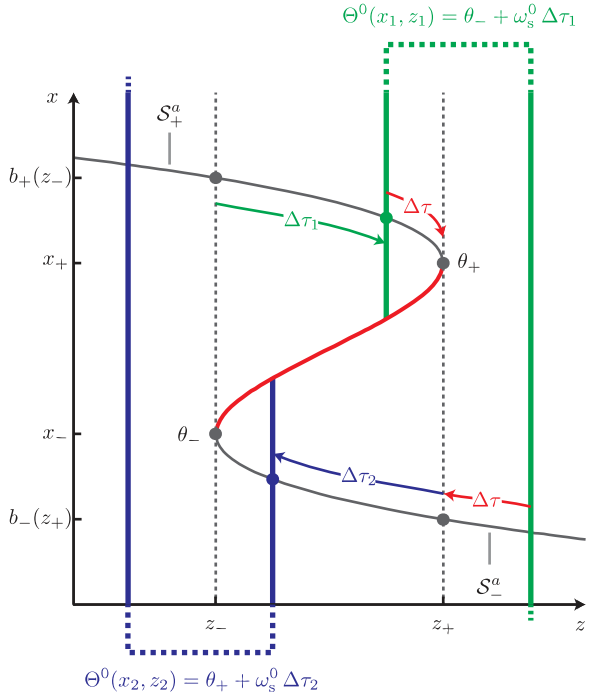

Fig. 3. Geometric construction of singular phase map. The phase map associates with each point on the periodic orbit a phase which corresponds to the normalized time $\omega_{\mathrm{s}}^0\,\Delta\tau$ required to reach this point from the reference position (x_-, z_-). For points on the lower branch, it is convenient to measure the normalized time from (x_+, z_+) and to add the phase $\theta_+ := \omega_{\mathrm{s}}^0\,\Delta\tau_+$. Because all points on a same vertical ray (in the bistable region) and converging to the same branch instantaneously jump on the branch in the singular limit, the phase map associates them with the same phase. In addition, other vertical lines (outside the bistable region) are associated with the same phase because these points converge in the same $\Delta\tau \pmod{T_{\mathrm{s}}^0}$ to (x_+, z_+). This vertical ray and these other vertical lines join 'virtually' at infinity. This is conceptually illustrated by the dotted line joining ray and lines associated with the same asymptotic phase.

corresponds to the remaining flowing time on the lower branch. To simplify notation, it is convenient to denote by $\Theta^0(x_+, z_+) =: \theta_+ = \omega_{\mathrm{s}}^0\,\Delta\tau_+$ the phase associated with the upper fold (and all points of the (weakly) unstable critical fiber joining (x_+, z_+) to $(b_-(z_+), z_+)$).

The notion of singular phase map can be extended to any point (x, z) in the basin of attraction of the singular periodic orbit. Because, in the singular limit, any singular trajectory starting from (x, z) instantaneously jumps from its initial condition to a branch of the critical manifold, all points on the same vertical line (that is, with the same value of slow variable z) that jump to the same branch are associated with the same phase.

- All points on the line $z = z_-$ (resp. $z = z_+$) are associated with the phase θ_- (resp. θ_+).
- For points with a slow variable in the bistable range, the asymptotic phase θ_1 of a point (x_1, z_1) belonging to the basin of attraction of the upper (resp. lower) branch is thus given by the phase θ_1 of the point at the intersection between the line $z = z_1$ and the upper (resp. lower) branch of the singular periodic orbit γ^0.
- In addition, all points outside the bistable range that converge to the upper fold in the same time interval

$\Delta\tau \pmod{T_s^0}$ as (x_1, z_1) are also associated with the asymptotic phase θ_1.

An elegant way to summarize the definition of the singular phase map is

$$\Theta^0(x,z) = \begin{cases} \theta_- + \omega_s^0\,\psi_+(z_-,z,0) \pmod{2\pi}, & \text{if (C1)},\\ \theta_+ + \omega_s^0\,\psi_-(z_+,z,0) \pmod{2\pi}, & \text{if (C2)}, \end{cases}$$

with

$$\text{(C1)} \equiv (x,z) \in \mathcal{B}(\mathcal{S}_+^a) \cup \mathcal{F}_+,$$
$$\text{(C2)} \equiv (x,z) \in \mathcal{B}(\mathcal{S}_-^a) \cup \mathcal{F}_-,$$

where $\psi_\bullet(z_0, z_\tau, \mathbf{0})$ (with $\bullet$ standing for $+$ or $-$) are functions that measure the time needed to travel along the critical manifold from the initial condition z_0 to final condition z_τ, and $\mathcal{B}(\mathcal{S}_\bullet^a)$ is the set of points that jumps to the stable branch $\mathcal{S}_\bullet^a$ of the critical manifold along the layer dynamics (3).

Singular isochrons are thus vertical lines for values of z outside the bistable range and vertical rays for values of z inside the bistable range. In the bistable region, vertical rays are separated by the repulsive branch $\mathcal{S}^r$ of the critical manifold. The vertical ray and the vertical lines associated with the same phase join 'virtually' at infinity (see Figure 3).

For constant inputs $u(\cdot) \equiv \bar{u}$, the function $\psi_\bullet(z_0, z_\tau, \bar{u})$ can easily be computed by integrating the reduced dynamics (4) on the stable branches of the critical manifold and they read

$$\psi_\bullet(z_0, z_\tau, \bar{u}) = \int_{z_0}^{z_\tau} \frac{1}{g(b_\bullet(\xi - \bar{u}), \xi)} d\xi,$$

i.e., the attractor is horizontally shifted by $-\bar{u}$.

Remark 2: We intentionally do not consider the unstable branch of the critical manifold $\mathcal{S}^r$ as being part of the basin of attraction of the singular periodic orbit. For small ϵ, this repulsive branch is perturbed into a repulsive set which has zero Lebesgue measure.

Remark 3: The singular periodic orbit γ^0 is parameterized by the map $x^\gamma : \mathbb{S}^1 \to \gamma^0$ that associates with each phase $\theta \in \mathbb{S}^1$ on the unit circle a point $(x^\gamma(\theta), z^\gamma(\theta))$ on the singular periodic orbit.

B. Singular (finite) phase response curves

We derive the singular (finite) phase response curve for two inputs: impulses, that is, $u(\cdot) = \alpha\,\delta(\cdot)$, and square pulses of finite duration, that is, $u(\cdot) = \bar{u}\,[1_+(\cdot) - 1_+(\cdot - \Delta)]$.

1) Impulse: An impulse $u(\cdot) = \alpha\,\delta(\cdot)$ induces a jump of the fast variable x in the fast-slow dynamics (3)–(4). The singular (finite) phase response curve is thus given by

$$Q^0(\theta; \alpha\,\delta(\cdot)) = \Theta^0(x^\gamma(\theta) + \alpha, z^\gamma(\theta)) - \theta.$$

As illustrated on Figure 4, if the impulse lets the state cross the unstable branch of the critical manifold (case 1), it produces a phase shift. In the opposite case (case 2), the state converges back to the initial condition almost instantaneously.

For simplicity, we assume monotonicity of this separatrix in the bistable region (that is, $(\partial b_r/\partial z)(z) > 0$).

Given a positive impulse of amplitude α, there exists a critical value $z_c(\alpha)$ of the slow variable such that a trajectory

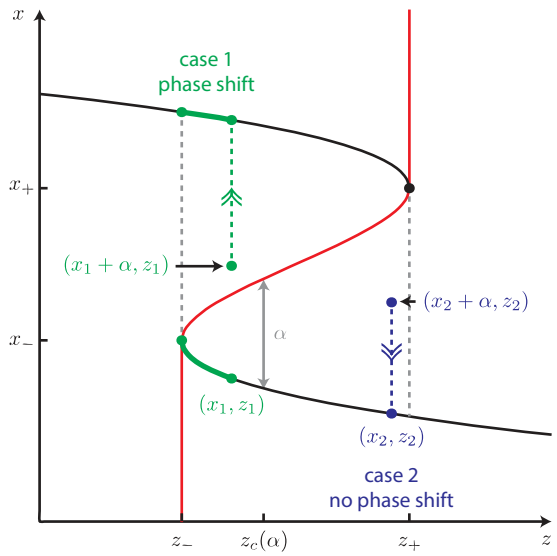

Fig. 4. Effect of positive impulses in the fast-slow dynamics (3)–(4). (Case 1) Close enough to the lower fold (on the lower branch), the reset state crosses the separatrix (red curve) and converges toward the upper branch instantaneously. The phase shift corresponds to the phase difference corresponding to the skipped portions of the singular periodic orbit (green). (Case 2) Far from the lower fold (on the lower branch) or on the upper branch, the reset state converges back to the initial state instantaneously. As a consequence, no phase shift is produced.

starting on the lower branch crosses the separatrix under the effect of the impulse for all z, such that $z_- \le z < z_c(\alpha)$. The critical value $z_c(\alpha)$ is given by

$$z_c(\alpha) = \{z \in \mathbb{R} : b_-(z) + \alpha = b_r(z)\}.$$

The asymptotic phase associated with this critical point $(b_-(z_c(\alpha)), z_c(\alpha))$ on the stable branch is denoted $\theta_c(\alpha)$. The phase shift $\Delta\theta$ induced by an impulse corresponds to the portion of singular periodic orbit skipped due to the impulse.

The phase response curve is given by

$$Q^0(\theta; \alpha\,\delta(\cdot)) = \begin{cases} \theta_- + \omega_s^0\,\psi_+(z_-, z^\gamma(\theta), 0) - \theta, & \text{if (C3)},\\ 0, & \text{o/w}, \end{cases}$$

where (C3) stands for $\theta_c(\alpha) < \theta \le \theta_-$.

Following a symmetric reasoning for negative impulses, that is, $u(\cdot) = -\alpha\,\delta(\cdot)$, the phase response curve is given by

$$Q^0(\theta; \alpha\,\delta(\cdot)) = \begin{cases} \theta_+ + \omega_s^0\,\psi_-(z_+, z^\gamma(\theta), 0) - \theta, & \text{if (C4)},\\ 0, & \text{o/w}, \end{cases}$$

where (C4) stands for $\theta_c(\alpha) < \theta \le \theta_+$ and $z_c(\alpha) = \{z \in \mathbb{R} : b_+(z) - \alpha = b_r(z)\}$.

2) Square pulse of finite duration: A square pulse of finite duration $u(\cdot) = \bar{u}\,[1_+(\cdot) - 1_+(\cdot - \Delta)]$ induces a behavior in the fast-slow dynamics (3)–(4) that is less trivial.

The phase response curve is given by

$$Q^0(\theta; u(\cdot)) = \Theta^0(x_\Delta(\theta), z_\Delta(\theta)) - (\theta + \omega_s^0\,\Delta_s^0), \qquad (5)$$

where $(x_\Delta(\theta), z_\Delta(\theta))$ is the state at time Δ_s^0 for the reduced dynamics starting from $(x^\gamma(\theta), z^\gamma(\theta))$ where Δ_s^0 is the pulse duration in the slow time scale and in the singular limit. It is

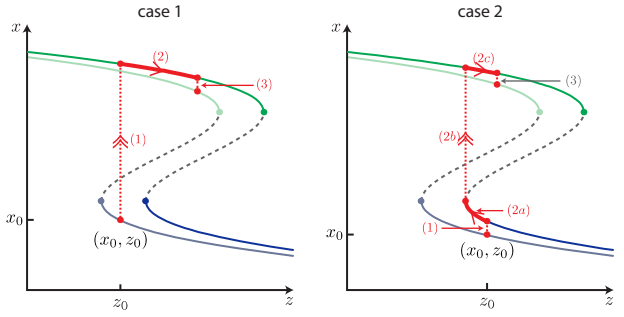

Fig. 5. Effect of positive square pulses of finite duration in the fast-slow dynamics (3)–(4). The state (x_Δ, z_Δ) of the trajectory starting from initial condition (x_0, z_0) (under a pulse of duration Δ) is graphically determined using functions $\psi_\bullet$ in order to predict the phase response associated with this pulse. The effect of a positive pulse is to shift temporally the critical manifold along the z-axis to the right. The singular trajectory starting from (x_0, z_0) evolves as follows: (1) jumps instantaneously on the shifted critical manifold, then (2) evolves around the shifted hysteresis (for a duration $\Delta = \Delta_a + \Delta_c$), and finally (3) jumps back to the initial critical manifold. The main difference between case 1 and case 2 is that during step (1) the trajectory converges to the opposite branch (with respect to the initial point) of the shifted critical manifold (in case 1) or to the same branch (with respect to the initial point) of the shifted critical manifold (in case 2).

thus necessary to compute the state (x_Δ, z_Δ) of the trajectory at the end of the pulse in order to compute the reset phase associated with its initial condition.

In the following, we describe how we can compute the state (x_Δ, z_Δ) using only the information contained in the functions $\psi_-(z_+ + \bar{u}, z, \bar{u})$ and $\psi_+(z_- + \bar{u}, z, \bar{u})$ (see Figure 5).

Starting from the initial condition (x_0, z_0) on the critical manifold, the trajectory evolves as follows (see Figure 5).

(1) Under a constant input $\bar{u}$, the critical manifold of the system is shifted along the z-axis. The singular trajectory jumps thus instantaneously to the branch of the "shifted critical manifold" corresponding to the basin of attraction to which the initial state belongs.
(2) Then, the trajectory evolves on the "shifted critical manifold", sliding slowly on branches and jumping instantaneously when it reaches "shifted folds".
(3) Finally, the trajectory jumps instantaneously back to the critical manifold at the end of the pulse.

Because the slow variable z is one-dimensional, the evolution of a trajectory under constant input $\bar{u}$ on an attractive branch is fully characterized by the functions $\psi_-(z_+ + \bar{u}, z, \bar{u})$ and $\psi_+(z_- + \bar{u}, z, \bar{u})$ during the flowing time. The total flowing time has to be equal to the duration Δ_s.

In Figure 5, we differentiate between two cases. In case 1, the initial condition on the *lower* branch of the critical manifold jumps directly to the *upper* branch of the shifted critical manifold. In case 2, the initial condition on the *lower* branch of the critical manifold jumps on the lower branch of the "shifted critical manifold". Case 1 produces larger phase shift than case 2.

Remark 4: The duration Δ is expressed in the fast time scale, that is, $\Delta_f^\epsilon = \Delta$. In the slow time scale, the duration is given by $\Delta_s^\epsilon = \epsilon\, \Delta_f^\epsilon$. We assume the duration of the pulse Δ_s^ϵ (in the slow time scale) do not tend to zero in the singular limit and thus that the duration Δ_f^ϵ tends to infinity. This assumption is motivated by the fact that the duration of the pulse is often a fraction of the period. So we may have $\lim_{\epsilon\to 0} \Delta_f^\epsilon = +\infty$ and $\lim_{\epsilon\to 0} T_f^\epsilon = +\infty$, and a finite ratio $\lim_{\epsilon\to 0} \Delta_f^\epsilon / T_f^\epsilon = C$ (with $C \neq 0$ and $C \neq \infty$).

VI. Application to a neural oscillator model

We illustrate our geometric approach on a simple neural oscillator model developed by FitzHugh [15] and Nagumo [16]. This model is a popular two-dimensional simplification of the Hodgkin-Huxley model of spike generation

$$\dot{v} = v - v^3/3 - w + I + u\,,$$
$$\tau\, \dot{w} = a - b\, w + v\,,$$

where v is the voltage variable, w is the recovery variable, and $\epsilon := 1/\tau$ is a small parameter.

A. Phase response curves for impulses

Figure 6A illustrates the (finite) phase response curve of the FitzHugh-Nagumo model for excitatory impulses $u(\cdot) = \alpha\, \delta(\cdot)$, with $\alpha > 0$. The solid line is the geometric prediction computed in the singular limit. Dots represent the phase response computed through numerical simulations of trajectories of the model for different values of the parameter ϵ.

The singular phase response curve is equal to zero except in one region of the periodic orbit which corresponds to the region right before the initiation of the upper part of the periodic orbit for an excitatory impulse. In this region, an impulse advances the initiation of the upper part of the periodic orbit. The phase advance decreases monotonically to zero until the phase corresponding to the lower fold.

For small values of ϵ, the geometric prediction matches very well the numerical phase response curves. For larger values of ϵ, the prediction still matches (qualitatively) the larger phase shifts arising before the lower fold but do not capture the small phase shifts arising before the upper fold.

B. Phase response curves for square pulses of finite duration

Figure 6B illustrates the (finite) phase response curve of the FitzHugh-Nagumo model for excitatory square pulses of finite duration. The solid line is the geometric prediction computed in the singular limit. Dots represent the phase response computed through numerical simulations of trajectories of the model for different values of the parameter ϵ.

The singular phase response curve is equal to zero except in two regions of the periodic orbit. The first region which exhibits the highest phase shifts corresponds to same region as for the impulse case. The phase shifts in this region follow a piecewise law: the breaking point in the phase shifts corresponds to the separation between initial conditions that continue to evolve on the shifted initial branch and those that directly jump to the opposite branch. The second region corresponds to point close to the other fold (see case 1 and case 2 in Figure 5). An excitatory pulse may delay the termination of the upper part.

Once again, for small values of ϵ, the geometric prediction matches very well the actual phase response curves. For larger

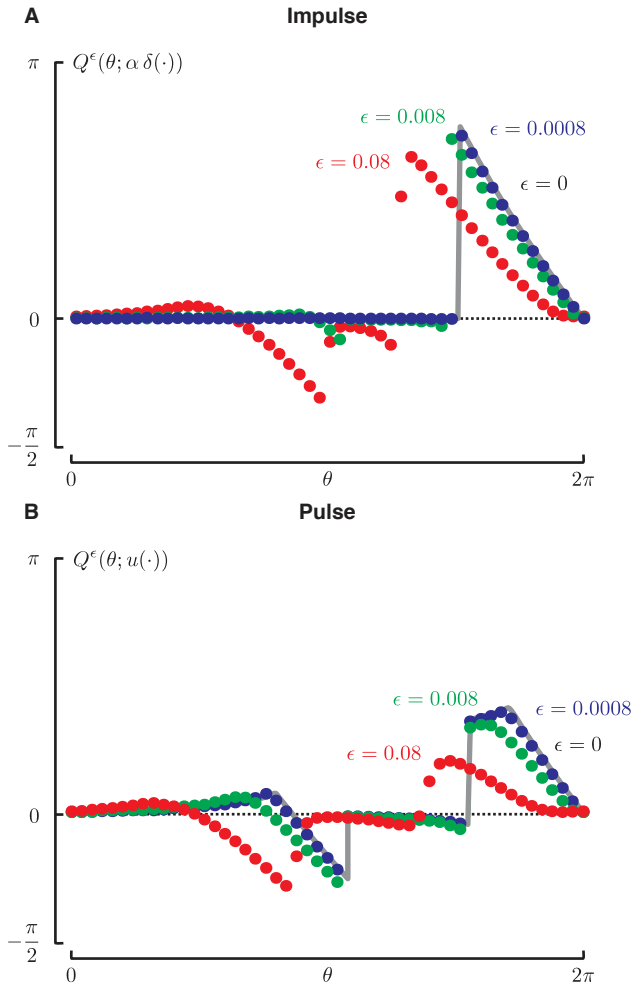

Fig. 6. (A) Phase response curves for excitatory impulses ($|\alpha| = 1.5$): singular geometric prediction (solid line) and numerical simulations (dots). (B) Phase response curves for excitatory pulses of finite duration ($|\bar{u}| = 0.25$, $\Delta = 0.1\,T$): singular geometric prediction (solid line) and numerical simulations (dots). (Parameter values: $a = 0.7$, $b = 0.8$, $I = 1$)

values of ϵ, the prediction matches qualitatively both non-zero regions of the phase response curve.

The main difference between the phase response curve for an impulse and for a pulse is that, close to the singular limit, a positive pulse may delay the termination of the behavior on the upper branch, while a positive impulse may not.

VII. Conclusion

We have introduced a novel methodology to construct globally the isochrons of relaxation oscillators close to the singular limit of infinite timescale separation between the oscillator variables. Based on this construction, we can approximate up to an order of the singular perturbation parameter the finite phase response curve of the relaxation oscillator for any perturbing input. We have illustrated this result for impulses and square pulses of finite duration.

The proposed construction complements the local approach of the classical infinitesimal phase response curve, which breaks down under too large timescale separation. On a more general bases, it allows to constructively predict the qualitative shape of the phase response curve of relaxation oscillators without the need of extensive numerical simulations. This property makes the proposed approach particularly appealing for control design.

Future work will aim at extending this analysis to more complex (higher dimensional) singularly perturbed oscillators, like bursters [13] or oscillators in circadian rhythms [17], and to oscillator synchronization studies, linking this result to fast threshold modulation phenomenon [18]. Also, we plan to provide rigorous persistence results based on the normal-form analysis contained in [12].

Acknowledgments

Rodolphe Sepulchre is gratefully acknowledged for insightful comments and suggestions.

References

[1] A. T. Winfree, *The Geometry of Biological Time*, 1st ed., ser. Biomathematics. New York, NY: Springer-Verlag, 1980, vol. 8.

[2] L. Glass and M. C. Mackey, *From Clocks to Chaos: the Rhythms of Life*. Princeton, NJ: Princeton University Press, 1988.

[3] D. V. Efimov, P. Sacré, and R. Sepulchre, "Controlling the phase of an oscillator: a phase response curve approach," in *Proc. 48th IEEE Conf. Decision and Control and 28th Chinese Control Conf.*, Shanghai, China, Dec. 2009, pp. 7692–7697.

[4] P. Danzl, J. Hespanha, and J. Moehlis, "Event-based minimum-time control of oscillatory neuron models: phase randomization, maximal spike rate increase, and desynchronization," *Biol. Cybern.*, vol. 101, no. 5–6, pp. 387–399, Dec. 2009.

[5] A. Mauroy, P. Sacré, and R. Sepulchre, "Kick synchronization versus diffusive synchronization," in *Proc. 51st IEEE Conf. Decision and Control*, Maui, HI, Dec. 2012, pp. 7171–7183.

[6] F. Dörfler and F. Bullo, "Synchronization in complex networks of phase oscillators: A survey," *Automatica*, vol. 50, no. 6, pp. 1539–1564, 2014.

[7] P. Sacré and R. Sepulchre, "Sensitivity analysis of oscillator models in the space of phase-response curves: Oscillators as open systems," *IEEE Control Syst. Mag.*, vol. 34, no. 2, pp. 50–74, Apr. 2014.

[8] E. M. Izhikevich, "Phase equations for relaxation oscillators," *SIAM J. Appl. Math.*, vol. 60, no. 5, pp. 1789–1804, 2000.

[9] N. Fenichel, "Persistence and smoothness of invariant manifolds for flows," *Indiana Univ. Math. J.*, vol. 21, no. 3, pp. 193–226, 1972.

[10] M. Krupa and P. Szmolyan, "Relaxation oscillation and canard explosion," *J. Differential Equations*, vol. 174, no. 2, pp. 312–368, Aug. 2001.

[11] P. Sacré, "Systems analysis of oscillator models in the space of phase response curves," Ph.D. dissertation, University of Liège, Belgium, Sep. 2013.

[12] J. Cannon and N. Kopell, "The leaky oscillator: Properties of inhibition-based rhythms revealed through the singular phase response curve," *SIAM J. Applied Dynamical Systems*, vol. 14, no. 4, pp. 1930–1977, 2015.

[13] A. Franci, G. Drion, and R. Sepulchre, "Modeling the modulation of neuronal bursting: A singularity theory approach," *SIAM J. Applied Dynamical Systems*, vol. 13, no. 2, pp. 798–829, 2014.

[14] E. M. Izhikevich, "Synchronization," in *Dynamical Systems in Neuroscience: the Geometry of Excitability and Bursting*. Cambridge, MA: The MIT Press, 2007, ch. 10.

[15] R. FitzHugh, "Impulses and physiological states in theoretical models of nerve membrane," *Biophys. J.*, vol. 1, no. 6, pp. 445–466, Jul. 1961.

[16] J. Nagumo, S. Arimoto, and S. Yoshizawa, "An active pulse transmission line simulating nerve axon," *Proc. IRE*, vol. 50, no. 10, pp. 2061–2070, Oct. 1962.

[17] P. Sacré and R. Sepulchre, "Sensitivity analysis of circadian entrainment in the space of phase response curves," in *A Systems Theoretic Approach to Systems and Synthetic Biology II: Analysis and Design of Cellular Systems*, V. V. Kulkarni, G.-B. Stan, and K. Raman, Eds. Springer Netherlands, 2014, pp. 59–81.

[18] D. Somers and N. Kopell, "Rapid synchronization through fast threshold modulation," *Biol. Cybern.*, vol. 68, no. 5, pp. 393–407, Mar. 1993.